

Spatial and temporal variability of ultrafine aerosol fraction (nanoparticles) in Siberia

M.Yu. Arshinov,¹ B.D. Belan,^{1,2} J.-D. Paris,³
G.O. Zadde,² and D.V. Simonenkov¹

¹*V.E. Zuev Institute of Atmospheric Optics,
Siberian Branch of the Russian Academy of Sciences, Tomsk, Russia*

²*Tomsk State University, Tomsk, Russia*

³*Laboratoire des Sciences du Climat et de l'Environnement IPSL,
CEA-CNRS, Saclay, France*

Received September 2, 2008

Spatio-temporal variability of the ultrafine and fine particle formation over Siberia is discussed. An estimate of foreground processes in the nanoparticle formation has been done. Analysis of the nucleation processes in the free atmosphere shows that nucleation events were observed in 85% of all airborne soundings performed over Siberia. In 80% of cases, nanoparticle layers are formed between heights of 4 and 7 km. The layer thickness mainly varies between 0.5 and 2.0 km and sometimes it can reach 4 km. A simultaneous increase in concentrations of nanoparticles and ozone, stated earlier, appears with an equal probability of coincidence or non-coincidence of nanoparticle and ozone layers at all heights. The horizontal length of nanoparticle layers varies between tens and 600 km. The most probable length is 100–300 km (> 50% of cases). Minimum of monthly mean values of both total nano- and nucleation mode particle concentrations in the ground layer is observed in summer. Concentration of particles with diameters between 3 and 70 nm in free troposphere varies from 300 in summer to 30 cm⁻³ in winter. The number density of bigger particles (70 < *d* < 200 nm) varies between 10 (in winter) and 30 cm⁻³ (in summer). Nucleation in the atmospheric boundary layer and free troposphere occurs absolutely independently. Main sources of nanoparticle formation in the free atmosphere are nucleation and photochemical processes. Contributions of nucleation, photochemical and advective processes in the atmospheric boundary layer are comparable.

Introduction

The ultrafine fraction (nanoparticles) is formed in air *in situ* by means of condensation from gas-precursors and starts the aerosol process in the atmosphere.¹ Therefore, to explain the behavior of aerosol in air in general it is necessary, first, to have an imagination about processes and scales of generation of this start fraction.

The design of instruments capable of detecting particles of 3–15 nm in size in the beginning of 90s of the 20th century resulted in active researches of nanoparticle formation processes in the atmosphere. The obtained results allow significant precision of the formation mechanisms in air. By now, it is ascertained in many *in situ* and laboratory experiments that nanoparticles can be formed by the following mechanisms: the binary nucleation, including water and sulphuric acid vapors; the ternary nucleation, including water, sulphuric acid, and ammonia vapors; the ion-induced nucleation; the particle formation during oxidation of organic compounds; the spontaneous condensation of organic compounds, the nucleation with participation of halogen compounds.

Despite the progress in study of nanoparticles, there are many ambiguities in understanding their part in atmospheric processes. As was shown in Ref. 2, this is caused by a lack of data on spatiotemporal scales of

generation of this fraction in various geographical regions and at different heights, its interaction with larger aerosol fractions and gaseous compounds. In addition, foreground mechanisms, participating in nanoparticles generation, change, depending on physical and geographical conditions. Thus, e.g., the halogen mechanism predominates in coastal areas, while it is low effective in continental conditions. The authors of Ref. 2 reviewed all the observation data obtained to 2004 and have shown that there is no any investigation over the immense territory of Russia throughout the troposphere among 124 projects, according to which the results of *in situ* measurements have been published.³ Thus, the immense part of the Earth territory is not covered by observational data. Hence, an estimate of the part of ultrafine fraction in atmospheric processes is virtually impossible without filling this gap.

Nanoparticles were measured in Russia mainly casually and locally^{4–9}; the only Ref. 7 has been mentioned in the above review. The measurements were carried out in courses of individual short-term experiments; therefore, they do not give a holistic notion about the behavior of nanoparticles in the ground layer.

In this work, data on spatiotemporal variability of ultrafine fraction generation over the significant part of Russian territory (Siberia) are presented and foreground mechanisms of nanoparticle generation are estimated.

1. Methods and material

To estimate spatial (horizontal and vertical) scales of regions where nanoparticles are generated, the "OPTIK-E" AN-30 aircraft-laboratory¹⁰ was used. It was equipped with a diffusive aerosol spectrometer (DAS) specially designed at the Institute of Chemical Kinetics and Combustion of SB RAS. The DAS allows measuring particle sizes within the 3–70 and 70–200 nm ranges. Meteorological parameters, the dispersion and chemical composition of submicron aerosol fraction, the gas component concentration, and the navigation performance were measured at the same time.¹⁰ In flights, the technique for determining the chemical composition of the ultrafine aerosol fraction with multilayer filters, elaborated in Karpov Institute of Physical Chemistry, was tried out.

The flight routes were Novosibirsk–Yakutsk–Novosibirsk and Novosibirsk–Salekhard–Khatanga–Chokurdakh–Pevek–Chokurdakh–Yakutsk–Mirny–Novosibirsk. The novel flying procedure was the following: the flight height varied all over the route from minimally possible (500 m) to the maximum equal to 7000 m. As a result, the section contains several vertical profiles (at a step of 50–250 km) with accounting for the horizontal component of the flight. The vertical section of a measured variable is built by the obtained data.

Thus, the areas of nanoparticle generation can be determined with a horizontal resolution of 50–250 km and vertical one of 50–100 m. The latter is determined by the ascent or descent speed, set by an air route

controller, and the DAS recording rate. The flight scheme according to the above procedure is shown in Fig. 1.

To study spatial distribution of nanoparticles of smaller scale, the mobile AKV-2 station was used, equipped with the same kit as the aircraft laboratory.¹¹ The working routes were Tomsk–Barnaul–Tomsk, Tomsk–Omsk–Tomsk, Tomsk–Irkutsk–Tomsk. In contrast to other mobile stations, AKV-2 allows measurements while moving, which gives a possibility to estimate microscale variations in the nanoparticle concentration as well.

Thus, the combination of two platforms for the measurement equipment allowed covering spatial scales from 3000 to several kilometers, i.e., from macro- to microscale intersecting at mesoscale.

Temporal scales were estimated in two ways. First, using the aircraft laboratory data, obtained every month while vertical sensing at the South of Western Siberia. Flights were carried out over the same region and with the same methodology. The second way consisted in routing (twenty-four-hour, hourly) measurements of concentrations of aerosol-forming gases (sulfur dioxide, hydrogen sulfide, ammonia, nitric oxide, and dioxide), sum hydrocarbons, gases participating in photochemical processes (ozone, carbon monoxide and dioxide, methane), ultrafine and submicron aerosol fractions; integral and UV solar radiation, meteorological parameters in two regions, i.e., background and urbanized. Such organization of measurements allows covering temporal scales from one season to several hours.

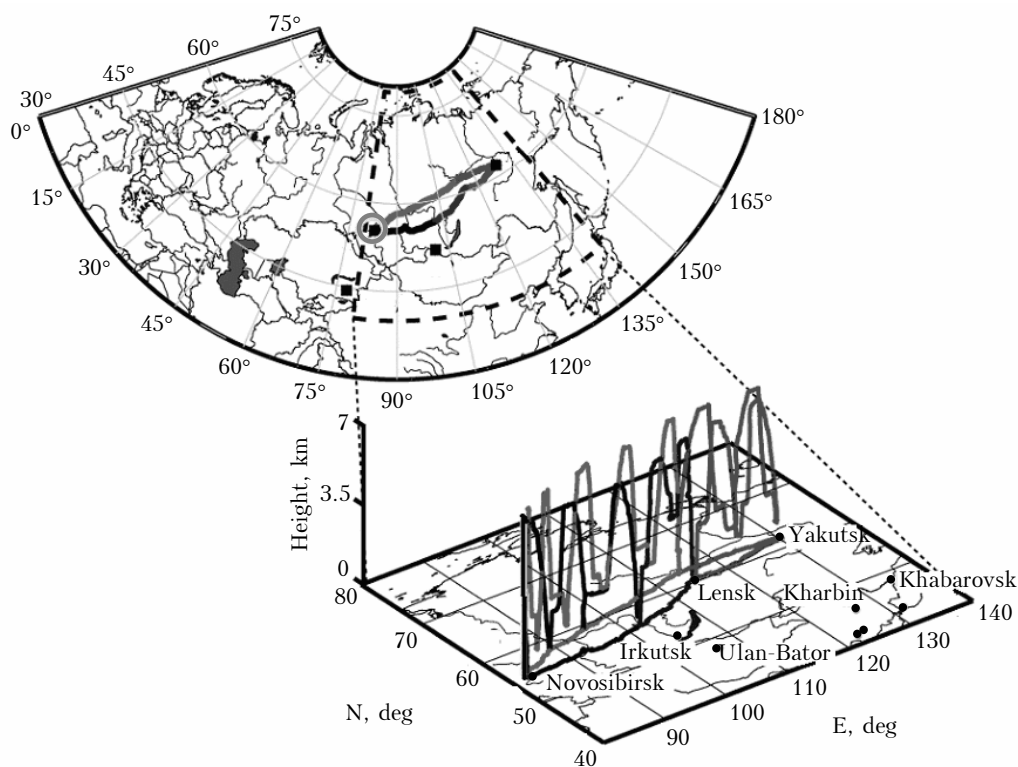


Fig. 1. The flight scheme in the YAK-AEROSIB project.

Contributions of different mechanisms in the particle nucleation were estimated by a novel technique.¹² The principle of the technique is the use of gas-precursor (sulfurous anhydride, ammonia, water vapor, concentrated hydrocarbons) measurement data for estimating the mechanism; intermediate components (hydroxyl) are calculated by the well-tested empirical relations, the calculation is controlled by the nanoparticle concentration and products of reactions. This approach allowed us to avoid additional expensive experiments and to be sure in reliability of qualitative conclusions. All the above-listed mechanisms work simultaneously in conditions of real atmosphere, and the same components can participate in different mechanisms at the same time; therefore, even measurements of all components cannot get rid of uncertainty when interpreting the results.

The obtained material is the following. Two-year routing monitoring of the fine fraction at the TOR-station (1996 and 2005–2006)^{13,14}, five flights Novosibirsk–Yakutsk–Novosibirsk, 64 vertical profiles around Novosibirsk, two flights Novosibirsk–Salekhard–Novosibirsk, and one flight Novosibirsk–Salekhard–Khatanga–Chokurdakh–Pevek–Chokurdakh–Yakutsk–Mirny–Novosibirsk. Several routes were carried out using the mobile station.

2. Spatial distribution of nanoparticles

Divide the consideration of the spatial distribution of the ultrafine aerosol fraction in the atmosphere into two parts: consider the vertical distribution by profiles, obtained during aircraft ascent and descent, and the horizontal one – on the basis of vertical sections, built by the data of vertical sounding when flying by the above routes.

2.1. Vertical distribution

First related casual experiments were carried out abroad in the middle of the 20th century. They gave only a general idea about vertical distribution of aerosol including the ultrafine fraction.¹⁵ In recent years, ultrafine aerosol particles are studied by teams of American researchers presenting different USA institutes and universities within different joint programs or projects.^{16–19} However, these teams carry out mainly aircraft investigations of nucleation and vertical distribution of aerosol in the atmosphere of equatorial area of the Pacific Ocean, which were first aimed at the study of cloud-formation processes. During last 5 years, they carried out a number of aerosol generation experiments in the free atmosphere of remote sea areas.

These experiments have shown^{16,18,19} that the nucleation could be sufficiently intensive in some conditions, up to appearance of aerosol layers where the concentration of ultrafine particles is larger than those in the ground layer. Groups of European researchers carried out the experiments over the

continent, but it was difficult to reveal natural processes of aerosol generation in the free troposphere by the experimental results due to a severe anthropogenic loading in Europe.^{20–22}

Our experiments²³ have shown that the nanoparticle concentration in the boundary atmospheric layer changes first by the Jaenicke model, while layers with an increased concentration are observed in the free troposphere. One can conclude that these layers are results of generation of new particles directly in the middle troposphere, since they and aerosol-forming compounds do not come from the lower layers. Their appearance cannot be explained by the long-range transport as well, because the lifetime of ultrafine particles ($d < 70$ nm) in the atmosphere is not large due to a high condensation growth rate.

The analysis of the concentration distribution of older and longer living particles ($d > 70$ nm) showed that it was lower as compared to newly generated ones and monotonely decreased virtually from the Earth's surface. At the long-range transport, concentrations of particles of $d < 70$ nm and $d > 70$ nm could be comparable since it would be enough time for generating the latter fraction.

The volume of data accumulated by now allows the estimation of the frequency of particle nucleation events in the free atmosphere and the frequency of coincidence of nanoparticle and ozone layers. It turned out that the nucleation in the free atmosphere was observed in 85% of cases, 45% of them were well pronounced and 40% – weak. In 15% of cases, the nucleation was not stated.

Vertical profiles are given in Ref. 23; therefore, consider statistical data. Repeatability of the ultrafine ($d < 70$ nm) aerosol fraction generation over south regions of the Western Siberia is shown in Fig. 2; it has been calculated by 64 vertical profiles.

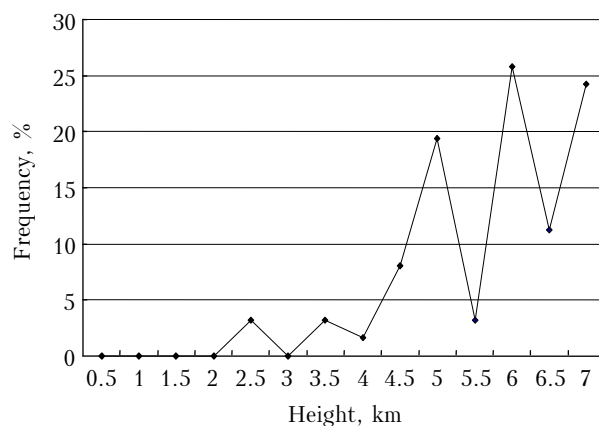


Fig. 2. Repeatability of nanoparticle generation layers at various heights.

As it is seen from Fig. 2, about 80% of particle layers are formed in the 4–7 km height range. Distinguishing of the layers is difficult inside the boundary atmospheric layer (below 2 km), because here could be plums of small fires. The uncertainty in

the origin of the increased particle concentration impels us to reject such cases. The downward excursions at heights of 5.5 and 6.5 km are incomprehensible since favorable conditions for particle generation at these and neighboring heights differ slightly.¹²

It is also interesting to consider data on the thickness of air layers, in which the nucleation is observed in the free troposphere (see Fig. 3).

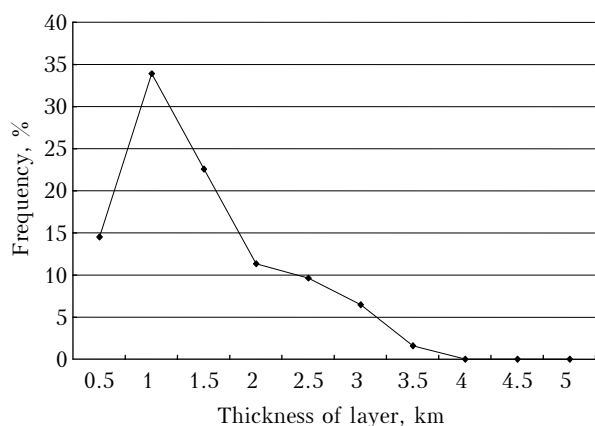


Fig. 3. Recurrence rate of the thickness of layers where nucleation occurs.

Figure 3 shows that the most frequent thickness of layer, where new particles are generated, is equal to 1 km (almost 35% of cases); the thickness can attain about 4 km, however it is from 0.5 to 2 km in 60% of cases.

It has been also registered that nanoparticle layers in the free atmosphere coincide with levels of increased ozone concentrations in the majority of flights. The frequency estimate shows that ozone and nanoparticle layers coincide for 72% of profiles. The height distribution is shown in Fig. 4.

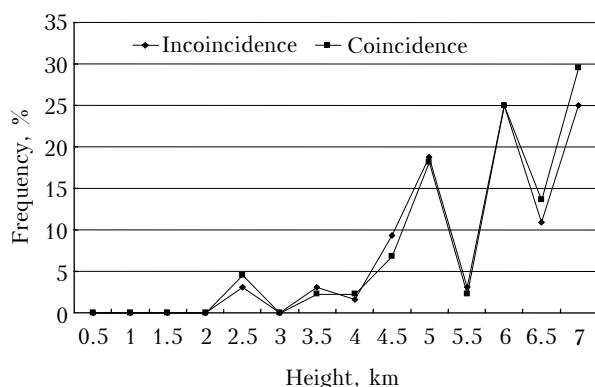


Fig. 4. Frequency of coincidence and incoincidence of layers of increased nanoparticle and ozone concentrations.

It is evident that the coincidence and incoincidence of nanoparticle and ozone layers have equal probability at all heights and generally repeat

the height variations of the frequency of nucleation layers. To our opinion, this evidences the fact that processes of generation of increased ozone and nanoparticle concentrations in the free atmosphere are the same.

The calculation²³ of vertical flows of the ultrafine and submicron fractions in the boundary layer and free atmosphere have shown that the middle troposphere is effectively separated from the particle source, i.e., the underlying surface. Positive flows, observed in the boundary layer, become negative when passing the upper boundary of the mixing layer. As a result, the nanoparticle concentration exponentially decreases from the Earth's surface to the boundary of the mixing layer down to its minimum.

2.2. Horizontal distribution

Consider the horizontal sizes of nanoparticle generation layers with the help of vertical cross-sections, built by the data of route measurements with a variable flight profile. An example of such cross section is shown in Fig. 5.

The top block shows the distribution of the accumulation mode of the ultrafine fraction, the middle one combines the nucleation and Aitken modes, and the bottom block shows the ozone distribution. The data on nanoparticles are shown in the form of logarithm due to a large range of their concentration variations.

It is seen that there are zones of the increased nanoparticle concentration in the free atmosphere, horizontal sizes of which can be determined. Table 1 is compiled by data of such profiles.

Table 1. Horizontal sizes of nanoparticles layers in the free atmosphere

Length, km	Frequency, %
< 100	11
100–199	26
200–299	32
300–399	16
400–499	11
500–599	5

Table 1 shows that the lengths of nanoparticle layers are from several tens to 600 km, the most probable is a length of 100–300 km (more than 50% of cases). Let the average wind speed be 10 m/s at these heights, then assessments of the process duration can be from 2 to 7 hours – the time required for the nanoparticle propagation to the obtained distances after the beginning of the nucleation process. This assessment is true if gas-precursors appeared at the height of new particle generation not in the form of the layer, in which the nucleation occurred simultaneously.

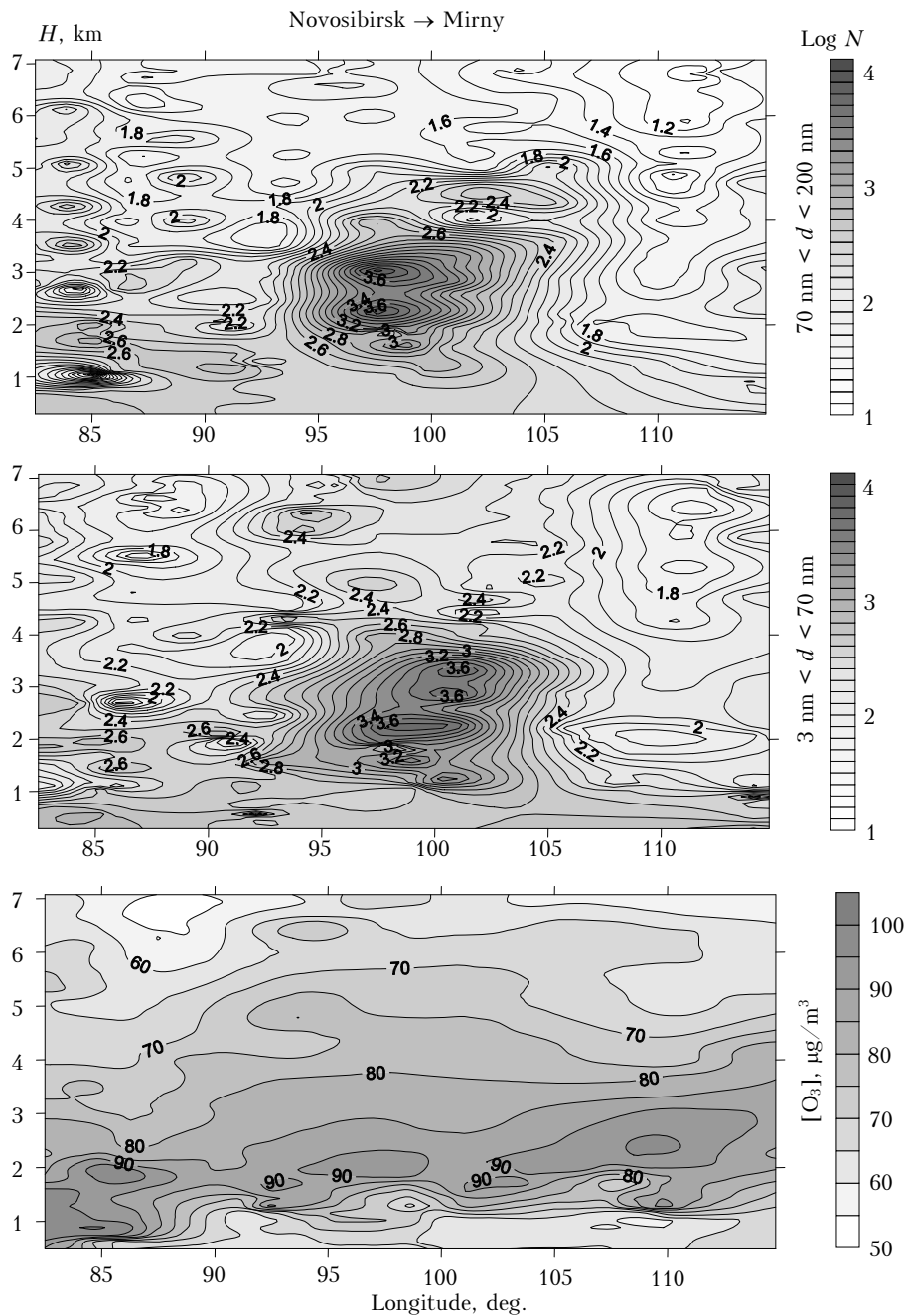


Fig. 5. Spatial distribution of nanoparticles and ozone concentrations (September 7, 2006).

3. Temporal variability

Begin the analysis of the temporal variability from annual variations of the ultrafine aerosol fraction. First consider the dynamics in the surface layer and then in the free troposphere.

The annual variations of the aerosol ultrafine fraction and nucleation mode are shown in Fig. 6.

The monthly mean minima of both total concentration of the ultrafine aerosol and particles of nucleation mode fall to summer months. Another feature of the annual variations is the appearance of one of the maxima in spring, and it can be considered

as characteristic, because it is pronounced in all curves shown in Fig. 6.

Estimates of the particle generation rate, made in Ref. 13, point out to the fact that nucleation processes do not weaken in summer, and particle-generation rates exceed winter values insignificantly. Hence, in view of locality of the processes *in situ*, it is possible to state that the intensity of the ultrafine aerosol generation has no strong seasonal dependence. At first sight, this seems to be illogical. The source of both primary aerosol and matters – precursors of the secondary aerosol is the underlying surface; therefore, it should be more “construction material” for the

ultrafine aerosol generation in summer. However, according to the classical nucleation theory,¹ the rate of stable nucleus generation strongly depends on the air temperature and is higher at lower temperatures.

At the same time, the large amount of vapors of aerosol-forming compounds in summer results in the increase in the nucleation rate and cluster mobility with simultaneous decrease in their sizes. The probability of the aerosol nanoparticle generation decreases significantly, because nuclei rapidly flow down to the atmospheric aerosol.

Thus, the character of the aerosol generation is relatively steady during a year, while the aerosol concentration in the surface layer is to be determined by the volume, where it is scattered, i.e., the height of the mixing layer. According to the data of the aircraft sounding over the Western Siberia,²⁴ the annual trend of the mixing layer height is opposite, with the maximum in summer months. This means that the surface concentration is diluted in summer due to turbulent redistribution of aerosol particles

in a large volume of air of the boundary atmospheric layer. Most likely, this circumstance affects the “spreading” of maximum in daily variations of total ultrafine fraction count concentration,¹³ since the height of the mixing layer in summer varies essentially during a day. To verify this fact, information on the vertical distribution of aerosol particles in the troposphere is required (Fig. 7).

It is seen from Figs. 7*a* and *b* that the concentration of particles of $d = 3\text{--}70$ nm varies from 300 in summer to 30 cm^{-3} in winter and of $d = 70\text{--}200$ nm – from 10 in summer to 30 cm^{-3} in winter. The variability of nanoparticles is higher in June and July because of the shorter lifetime in the atmosphere.^{25,26} The most important feature in Fig. 7 is the difference in concentrations of aerosol particles in the boundary layer and free atmosphere. Above the boundary layer, the concentration drops, though there is an intensive source of biogenic aerosol-forming vapors in this period, and the rate of the ion cluster generation is higher. This result is as yet unclear.

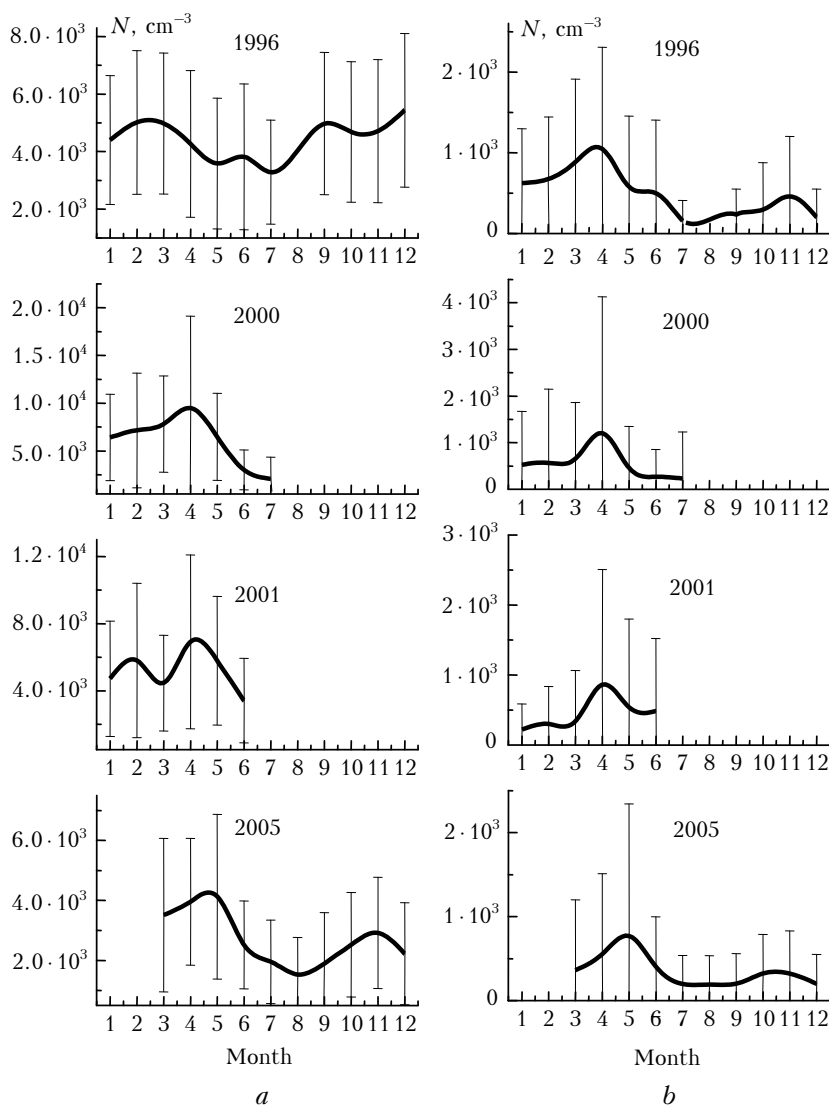


Fig. 6. Annual variations of the total (*a*) ultrafine aerosol count and concentration of particles of the nucleation mode (*b*).

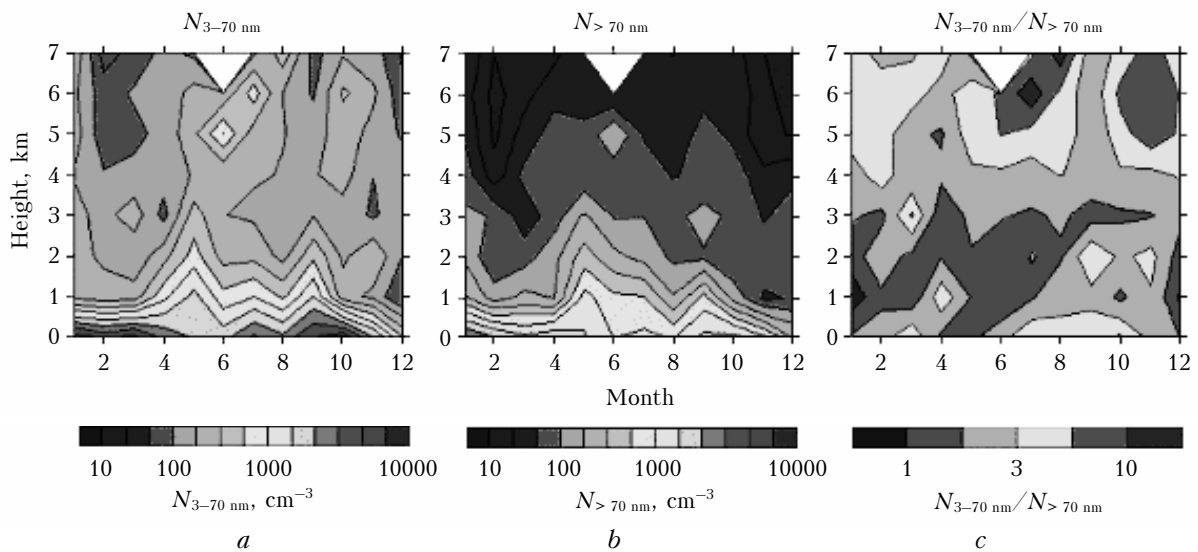


Fig. 7. Annual variations of the ultrafine fraction and accumulation mode of aerosol, as well as their ratios at different heights over the Western Siberia.

Figure 7c shows ratios of the modes at different heights during a year. They evidently vary from 0.1 to 10 in the free atmosphere. This probably indicates a random character in nucleation processes in the free atmosphere. The secondary maximum falls at November, which can well represent moldering processes in autumn.

The daily variations of the ultrafine fraction are well pronounced and described in detail in Ref. 13; therefore, we do not consider them here.

Among other time regularities, the 2-month as well as 3- and 7-day cycles can be distinguished. The last are rather caused by synoptical processes, i.e., mean lifetime of a cyclone or anticyclone and their couple. Shorter fluctuations have been recorded both by us and other teams,^{4–9} they can vary from several minutes to several hours. But their reliable statistics is absent as yet.

Table 2 presents the absolute maxima and minima of all measurements separately for the boundary atmospheric layer (BAL) and free troposphere (FT).

Table 2

$3 \text{ nm} < d < 70 \text{ nm}$	$N_{\min}, \text{ cm}^{-3}$	$N_{\max}, \text{ cm}^{-3}$
BAL	10	55455
FT	6	1536

4. Analysis of nucleation processes

Contributions of nucleation and photochemical processes in the particle generation were estimated by the measurement data of gas-precursors: sulfur dioxide, nitrogen oxide and dioxide, ozone, ultrafine and submicron aerosol fractions, UV radiation within the 295–310 nm range. We considered: the binary heteromolecular nucleation of sulfuric acid and water; the ternary nucleation of sulfuric acid, water, and ammonia; the binary nucleation of nitric acid

and water. First, the number of formed particles of 3 nm in diameter was calculated by the concentration of gases. The obtained value was compared with direct measurement data. A rate of $0.4\text{--}0.5 \text{ cm}^{-3} \cdot \text{s}^{-1}$ was obtained for the binary nucleation of H_2O and H_2SO_4 ; this value means that the binary nucleation cannot provide for the generation of the really observed number of nanoparticles. The addition of 0.05 ppb of NH_3 at the H_2SO_4 concentration, equal to 10^7 cm^{-3} , results in an increase in the rate up to $10 \text{ cm}^{-3} \cdot \text{s}^{-1}$. This value is close to really recorded rates of the nanoparticle generation in the atmosphere. At the same time, the calculation and comparison with direct measurements showed that the nitric acid participates in processes of heterogeneous condensation along with some volatile organic compounds rather than in processes of the homogeneous nucleation. A similar conclusion was made in Ref. 27, from which it follows that to attain significant nucleation rates at different variants of the ternary homogeneous nucleation with nitric acid, its concentration is to be not less than $10^{16}\text{--}10^{18} \text{ cm}^{-3}$, which is impossible in conditions of the Earth's atmosphere.

Conclusion

The analysis of nucleation processes in the free atmosphere showed that it was observed in 85% of cases of aircraft soundings, 45% of them were well pronounced and 40% were weak. Nucleation in the free atmosphere was not fixed in 15% of cases.

About 80% of particles layers are formed in a height range from 4 to 7 km. It is difficult to distinguish the layers in the ground layer below 2 km, because here can be plumes of small fires.

The most frequent thickness of a layer, where new particles are generated, is 1 km (about 35% of cases). The thickness can attain almost 4 km, but it lies in a range from 0.5 to 2 km in 60% of cases.

The simultaneous increase in nanoparticle and ozone concentrations, stated earlier, is expressed in the fact that a coincidence and an incoincidence of nanoparticle and ozone layers have equal probability at all heights and generally repeat the height dependence of the nucleation layer frequency. This witnesses the fact that the generation processes of increased concentrations of ozone and nanoparticles in the free atmosphere are the same.

The lengths of nanoparticle layers vary from several tens to 600 km; the most probable is a length of 100–300 km (> 50% of cases).

Minima of monthly mean values of both total concentration of the ultrafine aerosol and particles of the nucleation mode take place in summer months.

The free-atmosphere concentration of particles of $d = 3\text{--}70$ nm varies from 300 in summer to 30 cm^{-3} in winter and of $d = 70\text{--}200$ nm – from 10 in summer to 30 cm^{-3} in winter.

Nanoparticle nucleation processes in the boundary layer and free atmosphere are independent. The main sources of the nanoparticle generation in the free atmosphere are the nucleation and photochemical processes. In this case, measurement data have shown that contributions of the nucleation, photochemical and advective processes are comparable in the boundary atmospheric layer, riched by aerosol-forming vapors.

Acknowledgements

This work was supported by the Presidium RAS (Program No. 16), Earth Science Department of RAS (Programs Nos. 9 and 11), Russian Foundation for Basic Research (Grants Nos. 07–05–00645, 08–05–10033, and 08–05–92499), and ISTC (Projects Nos. 3032 and 3275).

References

1. N.A. Fuks, *Mechanics of Aerosols* (AS of the USSR, Moscow, 1955), 351 pp.
2. T. Petaja and M. Kulmala, eds., *Report Series in Aerosol Science* (Helsinki, 2006), No. 80, 82 pp.
3. M. Kulmala, H. Vehkamäki, T. Petäjä, M. Dal Maso, A. Lauri, V.-M. Kerminen, W. Birmili, and P.H. McMurry, *J. Aerosol Sci.* **35**, No. 2, 143–176 (2004).
4. A.S. Kozlov, A.N. Ankilov, A.M. Baklanov, E.D. Veselovskii, A.L. Vlasenko, S.I. Eremenko, S.B. Malyshev, S.E. Pashchenko, and A.V. Shitov, *Atmos. Oceanic Opt.* **11**, No. 6, 553–557 (1998).
5. A.S. Kozlov, A.N. Ankilov, A.M. Baklanov, A.L. Vlasenko, S.I. Eremenko, S.B. Malyshev, and S.E. Pashchenko, *Atmos. Oceanic Opt.* **12**, No. 12, 1046–1052 (1999).
6. V.V. Smirnov, J. Salm, J.M. Mäkelä, and J. Paatero, *Atmos. Oceanic Opt.* **17**, No. 1, 61–69 (2004).
7. P.K. Koutsenogii and R. Jaenicke, *J. Aerosol Sci.* **25**, No. 3, 377–383 (1994).
8. V.A. Zagainov, A.A. Lushnikov, Yu.G. Biryukov, T.V. Khodzher, A.E. Aloyan, and R. Arimoto, in: *Proc. of International Symp. "Aerosols and Safety"*, Obninsk (2005), pp. 38–40.
9. M.S. Cickishvili, V.A. Zagainov, V.M. Minashkin, G.I. Kardzhakhiya, A.G. Chkhartashvili, I.G. Shatberishvili, and T.L. Ninua, in: *Proc. of International Symp. "Aerosols and Safety"*, Obninsk (2005), pp. 43–45.
10. V.E. Zuev, B.D. Belan, D.M. Kabanov, V.K. Kovalevskii, O.Yu. Luk'yanov, V.E. Meleshkin, M.K. Mikushev, M.V. Panchenko, I.E. Penner, E.V. Pokrovskii, S.M. Sakerin, S.A. Terpugova, G.N. Tolmachev, A.G. Tumakov, V.S. Shamanaev, and A.I. Shcherbatov, *Atmos. Oceanic Opt.* **5**, No. 10, 658–663 (1992).
11. M.Yu. Arshinov, B.D. Belan, D.K. Davydov, G.A. Ivlev, A.V. Kozlov, D.A. Pestunov, E.V. Pokrovskii, D.V. Simonenkov, N.V. Uzhogova, and A.V. Fofonov, *Atmos. Oceanic Opt.* **18**, No. 8, 575–580 (2005).
12. M.Yu. Arshinov, B.D. Belan, and D.V. Simonenkov, *Atmos. Oceanic Opt.* **19**, No. 4, 292–303 (2006).
13. M.Yu. Arshinov and B.D. Belan, *Atmos. Oceanic Opt.* **13**, No. 11, 909–916 (2000).
14. M. Dal Maso, L. Sogacheva, M.P. Anisimov, M. Arshinov, A. Baklanov, B. Belan, T.V. Khodzher, V.A. Obolkin, A. Staroverova, A. Vlasov, V.A. Zagainov, A. Lushnikov, Y.S. Lyubovtseva, I. Riipinen, V.-M. Kerminen, and M. Kulmala, *Boreal Environ. Res.* **13**, No. 2, 81–92 (2008).
15. H. Weickmann, in: *Proc. of 1st Conf. Physics Clouds and Precipitation Particles*, H. Weickmann and W. Smith, eds. (Pergamon Press, New York, 1957), 81 pp.
16. A.D. Clarke, Z. Li, and M. Litchy, *Geophys. Res. Lett.* **23**, No. 7, 733–736 (1997).
17. A.D. Clarke, F.L. Eisele, V.N. Kapustin, K. Moore, D. Tanner, L. Mauldin, M. Litchy, B. Lienert, M.A. Carroll, and G. Albercook, *J. Geophys. Res. D* **104**, No. 5, 5735–5744 (1999).
18. A.D. Clarke, J.L. Varner, F.L. Eisele, R.L. Mauldin, D. Tanner, and M. Litchy, *J. Geophys. Res. D* **103**, No. 13, 16397–16409 (1998).
19. R.J. Weber, P.H. McMurry, R.L. Mauldin, III, D.J. Tanner, F.L. Eisele, A.D. Clarke, and V.N. Kapustin, *Geophys. Res. Lett.* **26**, No. 3, 307–310 (1999).
20. A. Keil and M. Wendisch, *J. Aerosol Sci.* **32**, No. 5, 649–660 (2001).
21. C.A. Brock, F. Schröder, B. Kärcher, A. Petzold, R. Busen, and M. Fiebig, *J. Geophys. Res. D* **105**, No. 21, 26555–26567 (2000).
22. C.A. Brock, R.A. Washenfelder, M. Trainer, T.B. Ryerson, J.C. Wilson, J.M. Reeves, L.G. Huey, J.S. Holloway, D.D. Parrish, G. Hübler, and F.C. Fehsenfeld, *J. Geophys. Res. D* **107**, No. 12, doi: 10.1029/2001JD001062 (2002).
23. M.Yu. Arshinov and B.D. Belan, *Atmos. Oceanic Opt.* **17**, No. 7, 489–499 (2004).
24. B.D. Belan, *Atmos. Oceanic Opt.* **7**, No. 8, 558–562 (1994).
25. B.T. Jobson, S.A. McKeen, D.D. Parrish, F.C. Fehsenfeld, D.R. Blake, A.H. Goldstein, S.M. Schauffler, and J.C. Elkins, *J. Geophys. Res. D* **104**, No. 13, 16091–16113 (1999).
26. L.H. Young, D.R. Benson, W.M. Montanaro, S.H. Lee, L.L. Pan, D.C. Rogers, J. Jensen, J.L. Stith, C.A. Davis, T.L. Campos, K.P. Bowman, W.A. Cooper, and L.R. Lait, *J. Geophys. Res.* **112**, doi:10.1029/2006JD008109 (2007).
27. I. Napari, M. Kulmala, and K.H. Vehkamäki, *J. Chem. Phys.* **117**, No. 18, 8418–8425 (2002).